

Performance and discharge characteristics of doped (beta) MnO_2 in H_2SO_4 electrolyte

Buqui D. Desai*, Fernando S. Lobo and V.N. Kamat Dalal

Department of Chemistry, Goa University, P.O. Box, Bambolim 403 202, Goa (India)

(Received April 2, 1993; in revised form January 17, 1994; accepted January 21, 1994)

Abstract

Doped manganese dioxides ($\beta\text{-MnO}_2$) were prepared by thermal decomposition (180 °C) of manganese nitrate in the presence of weighed quantities of NH_4VO_3 , $\text{Na}_2\text{WO}_4 \cdot 2\text{H}_2\text{O}$, LiNO_3 , AgNO_3 or MoO_3 . Detailed chemical analyses, surface area and pycnometric density determinations were carried out, and the electrochemical performance was evaluated in H_2SO_4 (8 N) electrolyte. The discharge behaviour was monitored using constant currents and constant resistances (both continuous and intermittent discharge). Some of the Mo-doped samples together with the Li- and Ag-doped materials performed well as cathodes in H_2SO_4 . The consistency of discharge duration under different discharge regimes was a marked feature of the behaviour of some of the compositions.

Introduction

A small amount of fundamental work has been reported on the discharge of manganese dioxide in acid solution [1, 2]. Of the mineral acids only sulfuric acid can be used. Other acids have been ruled out, nitric acid because it is too corrosive, and hydrochloric acid because of its direct chemical reaction with MnO_2 liberating chlorine. MnO_2 has been primarily used as the cathode material in the Leclanché cell, which can be written schematically as $\text{MnO}_2/(\text{ZnCl}_2\text{-NH}_4\text{Cl})\text{aq}/\text{Zn}$. Valand [3] reported that there was a considerable improvement in the discharge behaviour of the MnO_2 electrode when it included up to 1% MoO_3 . Valand and Coleman [4] reported that the zinc-manganese dioxide acid battery has a relatively flat discharge at high voltage. In a single-cell discharge at a current drain of about 10 mA cm^{-2} , good utilization of the MnO_2 occurred at 2.0 to 1.9 V. The electrolyte in these primary batteries is 6 N to 8 N H_2SO_4 . The cathode used in reserve primary cell is an anodized lead or a lead alloy current collector which is coated with a mixture of MnO_2 , graphite, and carboxymethyl cellulose (CMC), amalgamated zinc metal sheet being used as an anode. Coleman *et al.* [5] proposed a reserve primary cell system where the electrolyte is H_2SO_4 and the zinc anode is amalgamated to reduce the corrosion which takes place even on open circuit. The reserve primary cell has an open-circuit potential of nearly 2.2 V and the working voltage on moderate drain starts at 2.0 to 2.05 V. A large fraction of the active material is used over a 10% voltage drop from 2.0 to 1.8 V. The aim of the present investigation was primarily to assess the performance of $\beta\text{-MnO}_2$ -containing various dopants as cathode materials on the lines suggested by Valand

*Author to whom correspondence should be addressed.

and Coleman [4]. A secondary objective was to check the reproducibility of Mo-doped samples under different discharge regimes.

Experimental

Sample preparation

Doped manganese dioxides were prepared by the procedure of Valand [3]. The salts taken for doping were similar to those used by Rophael *et al.* [6]. All samples were prepared by thermal decomposition of $\text{Mn}(\text{NO}_3)_2 \cdot 4\text{H}_2\text{O}$ intimately mixed with the dopant salt in air at 180 °C for 5 days. After decomposition, the oxide was ground to pass a 200 mesh sieve. The powder was washed with distilled water several times except in the case of the molybdenum- and vanadium-doped samples where 7.5 N ammonia solution was added to the oxide and stirred for 30 min for the removal of unreacted molybdenum as ammonium molybdate and precipitated unoxidized manganese ions as manganese hydroxide. The oxides were then washed with water and dried at 110 °C to constant weight and stored over P_2O_5 in a desiccator. The quantities of the reagents used for the oxide preparation are presented in Tables 1 and 2. The dopants were estimated by using atomic absorption spectrophotometer (AAS) and also by energy dispersive X-ray fluorescence (EDXRF). The results are presented in Table 1.

Sample characterization

X-ray powder diffraction (XRD) measurements were made using nickel-filtered Cu $K\alpha$ radiation ($\lambda = 1.54 \text{ \AA}$), over a range from 10 to 80 degrees 2θ (2° , $2\theta/\text{min}$). The principal phase in all the materials was $\beta\text{-MnO}_2$. The XRD data of the representative samples is presented in Table 3.

Pycnometric density measurements were carried out using a 25 ml density bottle with white kerosene at 40 °C under vacuum [10].

The surface area of the samples was determined by zinc ion adsorption (ZIA method) [9].

The activity index of the samples was determined by the hydrazine method of evaluating the activity [8].

Cell assembly and electrode preparation

1.5 g samples of the dry mix in the proportion 85:15 by weight of MnO_2 materials to graphite were prepared. A solution of 5 g CMC disodium salt in 300 ml H_2O (1.67% w/v) was prepared. The dry mix was then blended with 0.65–0.75 ml of the CMC solution following the procedure recommended by Valand and Coleman [4]. Current collectors were anodized in 8 N H_2SO_4 at 120 mA for 2.5 min with a 2.54 cm \times 2.54 cm perforated lead foil (0.012 cm thick). The active cathode material was pasted on both sides of the anodized foil, dried for about 1 h in air and then compressed at 7 tons load. After being cleaned in alkali to remove any surface oil film zinc sheets were washed and amalgamated by brief exposure to a dilute solution of mercuric chloride in water. The amalgamated zinc sheets served as anode materials (counter and reference electrodes).

Experimental

One cathode and two zinc anodes were assembled into a cell, physical separation being maintained by an expanded polypropylene mesh (see Fig. 1). The cell was

TABLE 1
Preparation and chemical analyses data

Sample	Quantities of reagents used in the preparation of samples	Dopant ^a (wt.%)	Dopant ^b (wt.%)	MnO ₂ (wt.%)	Mn (wt.%)	x in MnO _(1+x)	Combined H ₂ O y (%) [7]	Activity index [8]	Surface area (Z/A) [9] (m ² g ⁻¹)
S ₀	200.8 g Mn(NO ₃) ₂ ·4H ₂ O			98.43	63.18	0.9846	0.20	26.60	8.75
S ₂	175.7 g Mn(NO ₃) ₂ ·4H ₂ O + 10.08 g MoO ₃	2.35 Mo	2.64 Mo	81.48	64.55	0.7977	3.10	21.55	24.50
S ₃	150.6 g Mn(NO ₃) ₂ ·4H ₂ O + 0.864 g MoO ₃	1.10 Mo	1.05 Mo	93.48	61.80	0.9559	1.10	26.45	26.25
S ₄	175.7 g Mn(NO ₃) ₂ ·4H ₂ O + 0.1008 g MoO ₃	0.12 Mo	0.12 Mo	95.40	65.92	0.9146	0.70	55.00	24.50
S ₅	200.8 g Mn(NO ₃) ₂ ·4H ₂ O + 0.04 g MoO ₃	0.03 Mo	0.03 Mo	96.70	64.02	0.9546	0.50	58.00	29.00
Li-1	200.8 g Mn(NO ₃) ₂ ·4H ₂ O + 55.16 g LiNO ₃		0.03 Li	99.65	62.14	1.0000	0.30	57.00	60.50
Li-2	200.8 g Mn(NO ₃) ₂ ·4H ₂ O + 5.516 g LiNO ₃		0.06 Li	97.94	63.18	0.9797	0.60	60.00	70.60
Ag-1	175.7 g Mn(NO ₃) ₂ ·4H ₂ O + 1.189 g AgNO ₃	1.01 Ag	1.02 Ag	87.10	56.31	0.9775	2.60	48.50	55.00
Ag-2	175.7 g Mn(NO ₃) ₂ ·4H ₂ O + 11.8909 g AgNO ₃	9.05 Ag	9.90 Ag	88.84	54.94	1.0000	1.80	53.26	59.50
W	200.8 g Mn(NO ₃) ₂ ·4H ₂ O + 2.6388 g Na ₂ WO ₄ ·2H ₂ O	2.95 W	3.05 W	94.04	60.43	0.9835	0.80	30.00	96.25
V	175.7 g Mn(NO ₃) ₂ ·4H ₂ O + 8.1886 g NH ₄ VO ₃		5.30 V	82.02	59.06	0.8776	1.60	52.00	110.25

^a% Dopant estimated by EDXRF.

^b% Dopant estimated by AAS.

TABLE 2

Quantities of manganese and dopants present in moles

Sample	Moles of Mn taken for doping	Moles of dopant initially taken for doping	Moles of dopant present in sample	Moles of dopant lost in washing
S ₀	0.8			
S ₂	0.7	4.66×10^{-2}	0.11×10^{-2}	4.56×10^{-2}
S ₃	0.6	4.00×10^{-3}	1.45×10^{-3}	2.55×10^{-3}
S ₄	0.7	4.66×10^{-4}	4.48×10^{-4}	0.18×10^{-4}
S ₅	0.8	1.82×10^{-4}	1.35×10^{-4}	0.47×10^{-4}
Li-1	0.8	8.05×10^{-2}	0.02×10^{-2}	8.02×10^{-2}
Li-2	0.8	8.05×10^{-3}	0.59×10^{-3}	7.46×10^{-3}
Ag-1	0.7	7.00×10^{-3}	3.45×10^{-3}	3.55×10^{-3}
Ag-2	0.8	4.44×10^{-2}	3.48×10^{-3}	0.97×10^{-2}
W	0.8	4.45×10^{-3}	0.39×10^{-3}	4.06×10^{-3}
V	0.7	3.05×10^{-3}	2.96×10^{-2}	0.09×10^{-2}

TABLE 3

X-ray diffraction data and lattice parameters of a few representative samples

S ₀		Li-2		V		Ag-2	
<i>d</i> (nm)	<i>I/I</i> ₀						
0.308	100	0.311	100	0.311	53	0.307	80
0.239	84	0.270	5	0.241	100	0.239	100
0.234 ^a		0.239	73	0.235 ^a		0.233 ^a	
0.219	17	0.234 ^a		0.220	20	0.220	18
0.210	34	0.218	13	0.211	51	0.210	36
0.202 ^a		0.211	31	0.202	54	0.202 ^a	
0.196	7	0.202 ^a		0.162	74	0.162	75
0.161	80	0.196	8	0.143	56	0.155	26
0.155	26	0.162	73	0.130	26	0.143	52
0.143	25	0.155	22	0.122	49	0.139	9
0.140	5	0.143	18			0.130	30
0.138	11	0.138	10			0.122	61
0.130	31	0.130	80				
<i>a</i> = 0.4382 nm		<i>a</i> = 0.4389 nm		<i>a</i> = 0.4448 nm		<i>a</i> = 0.4382 nm	
<i>c</i> = 0.2864 nm		<i>c</i> = 0.2882 nm		<i>c</i> = 0.2871 nm		<i>c</i> = 0.2872 nm	

^aTraces of γ -Mn₂O₃.

activated by immersion in a 100 ml solution of 8 N H₂SO₄ for 30 min. The electrodes were allowed to stabilize on open circuit before they were discharged at a constant current of 60 mA, (4.65 mA cm⁻²) at room temperature (28 °C) and at 0 °C. The cell was also discharged at 120 mA, (9.30 mA cm⁻²) at room temperature (28 °C). The results of the discharge performances are presented in Tables 4 and 5 and the plots of discharge duration versus closed-circuit voltage are depicted in Figs. 2

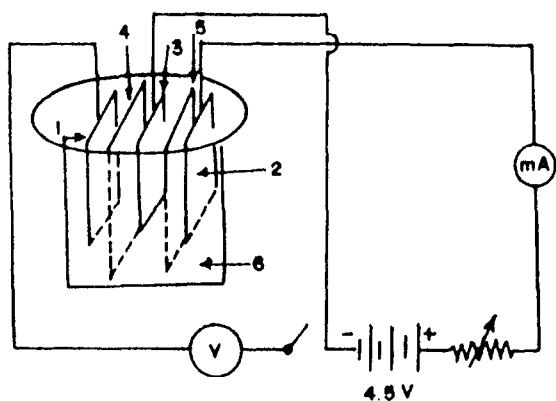


Fig. 1. Circuit diagram of the cell for discharge in H_2SO_4 electrolyte. (1) zinc reference electrode; (2) zinc counter electrode; (3) MnO_2 cathode; (4) and (5) expanded polypropylene mesh (separator), and (6) 8 N H_2SO_4 (electrolyte).

to 7. The cell was also discharged continuously using $10\ \Omega$ fixed resistance till a cutoff voltage of 1.0 V versus Zn. The relevant data are given in Table 6. The samples were also discharged at $10\ \Omega$ intermittent discharge, 0.5 h/day at room temperature ($28\ ^\circ\text{C}$). The results are presented in Table 6.

Results and discussion

Discharge under constant current of 60 and 120 mA

The sample S_5 containing the least amount of molybdenum appears to give by far the best performance from amongst the molybdenum-doped materials. The maximum effective service is delivered by the lithium-doped Li-2, silver-doped Ag-2 and vanadium-doped V- MnO_2 samples. In the case of V- MnO_2 sample, the discharge time at $28\ ^\circ\text{C}$ is 6.16 h and at $0\ ^\circ\text{C}$ it is 5.50 h. The energy density being $116\ \text{Wh kg}^{-1}$ at $28\ ^\circ\text{C}$ and $76\ \text{Wh kg}^{-1}$ at $0\ ^\circ\text{C}$. The discharge of V- MnO_2 is well sustained both in terms of mAh obtained and energy density as compared with the rest of the samples (see Table 4). Li-2 shows an efficiency of more than 100% in both the discharge regimes (i.e., at 60 and 120 mA). If 1.5 g of 85% MnO_2 (as in the 85:15 wt.% dry mix) is discharged at 60 mA, the theoretical time for one-electron discharge (i.e., for reduction of MnO_2 to a valence of 3) is 6.55 h, assuming MnO_2 to be stoichiometric; 6.55 h is thus taken as the maximum theoretical capacity. On the other hand, the efficiency of S_5 , V- MnO_2 and Ag-2 decline perceptibly under high current drain (120 mA). It is seen from the Table 4 that the percentage efficiency in all the samples decreases when the 60 mA discharge is carried out at $0\ ^\circ\text{C}$.

Discharge under constant resistance ($10\ \Omega$)

There are two different discharge regimes: (i) continuous discharge, and (ii) intermittent discharge (0.5 h/day).

The values of the theoretical Ah capacity calculated on the basis of Ruetschi's [11] and Atlung's [12] methods are presented in Table 7. The expected Ah capacity was computed from the formula proposed by Huber [13] for Leclanché cells:

$$\text{Ah}_{\text{expected}} = \text{Ah}_{\text{theoretical}} [1 - \exp(-KR^{1/2})] \quad (1)$$

TABLE 4
Discharge characteristics in 8 N H₂SO₄, 60 mA

Sample	At room temperature (28 °C)						At 0 °C					
	Discharge time (h)	Usable energy (J g ⁻¹)	Energy obtained (C g ⁻¹)	Energy density (Wh kg ⁻¹)	Efficiency (%)	Discharge time (h)	Usable energy (J g ⁻¹)	Energy obtained (C g ⁻¹)	Energy density (Wh kg ⁻¹)	Efficiency (%)		
S ₀	5.33	387	903	107	81	4.66	246	789	68	71		
S ₂	4.50	330	762	92	69	2.50	110	424	31	38		
S ₃	6.00	460	1016	128	92	4.50	302	762	84	69		
S ₄	5.66	418	959	116	86	5.16	311	874	86	79		
S ₅	5.75	421	974	117	88	4.50	277	762	77	69		
Li-1	4.66	333	789	93	71	2.33	138	395	38	36		
Li-2	6.66	494	1128	137	102	4.33	251	734	70	66		
Ag-1	4.33	316	734	88	66	2.00	152	339	42	31		
Ag-2	5.50	373	932	104	84	4.33	195	734	54	66		
W	4.66	376	789	104	71	3.00	212	508	59	46		
V	6.16	418	1044	116	94	5.50	274	932	76	84		

TABLE 5

Discharge characteristics in 8 N H₂SO₄, at (120 mA), room temperature (28 °C)

Sample	Discharge time (h)	Usable energy (J g ⁻¹)	Energy density (Wh kg ⁻¹)	Energy obtained (C g ⁻¹)	Efficiency (%)
S ₀	2.45	277	77	830	75
S ₂	2.16	237	66	732	66
S ₃	1.33	147	40	451	41
S ₄	2.83	435	121	959	86
S ₅	3.00	469	130	1016	92
Li-1	2.33	311	86	789	71
Li-2	3.33	508	141	1128	102
Ag-1	1.83	232	64	620	56
Ag-2	2.16	294	82	732	66
W	2.33	282	78	789	71
V	3.00	452	125	1016	92

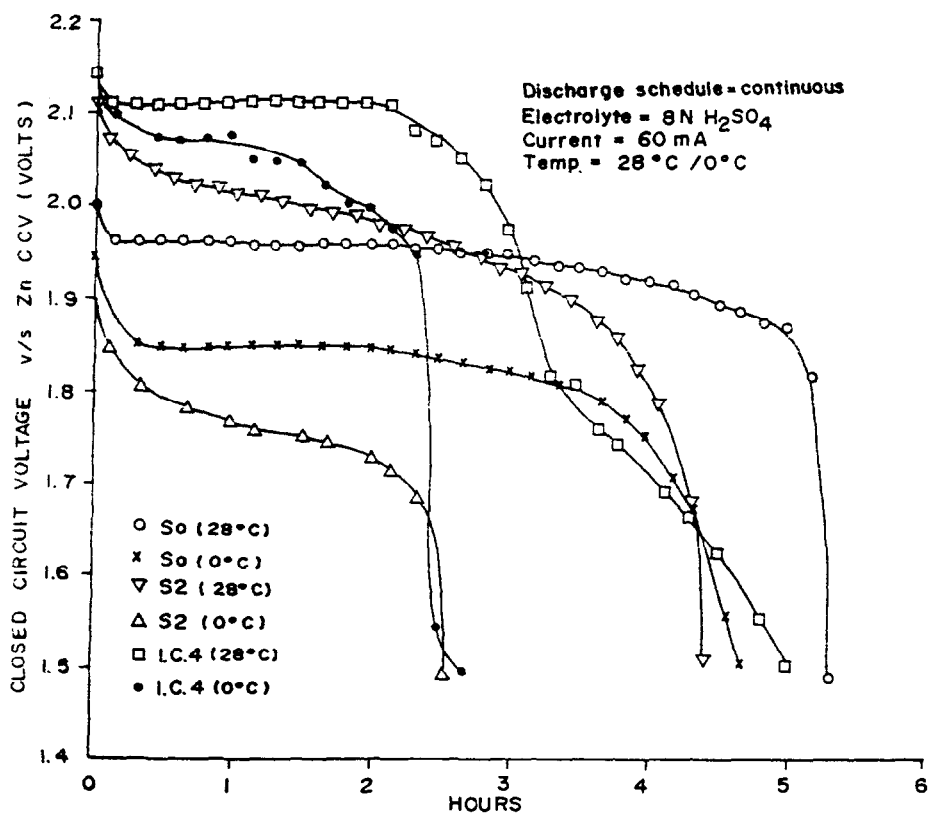


Fig. 2. Plots of closed-circuit voltage vs. time.

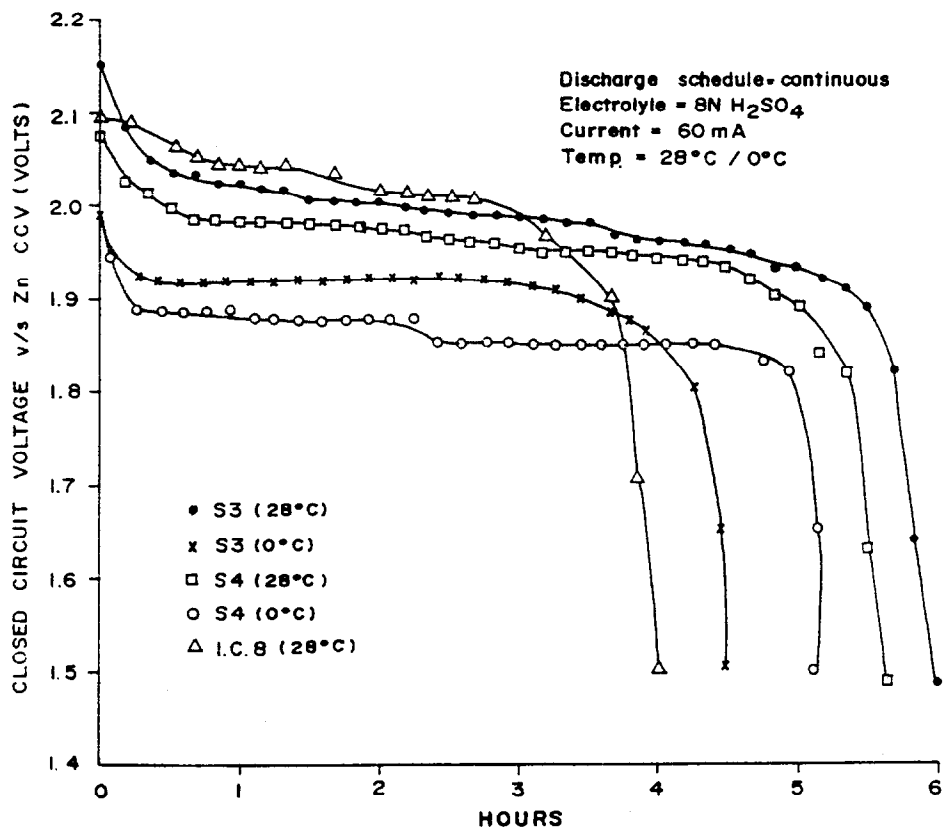


Fig. 3. Plots of closed-circuit voltage vs. time.

The value of the constant K which turns out to be 0.2 in the case of commercial dry cells, on account of its geometry, is here taken to be equal to unity as the electrodes used in this work were planar and in the form of porous paste. The value of unity for K is a rough approximation since K is a constant characterizing the physical and chemical properties of the electrodes; R represents the polarizing effect of the current and the index $1/2$ indicates that diffusion processes are the major components of the polarization processes [13]. The values of the discharge capacities are also tabulated in Table 6.

The current was recorded throughout the discharge period from time to time at specific intervals and the average of this was then taken to calculate the observed discharge capacity. The percentage utilization was obtained by assuming the expected Ah to be 100%. Li-2 and Ag-2 which contain more lithium and silver respectively, have greater capacities than Li-1 and Ag-1. This trend is opposite to the trend exhibited by the molybdenum-doped family in which S₅ containing the least amount of molybdenum shows the best discharge performance. It needs to be emphasized that the values of surface area [9] and the activity index [8] reflect the trend observed in Table 1 in the sense that the lower the values of molybdenum present the higher are the available % MnO₂, activity index and surface area, but silver- and lithium-doped MnO₂ show

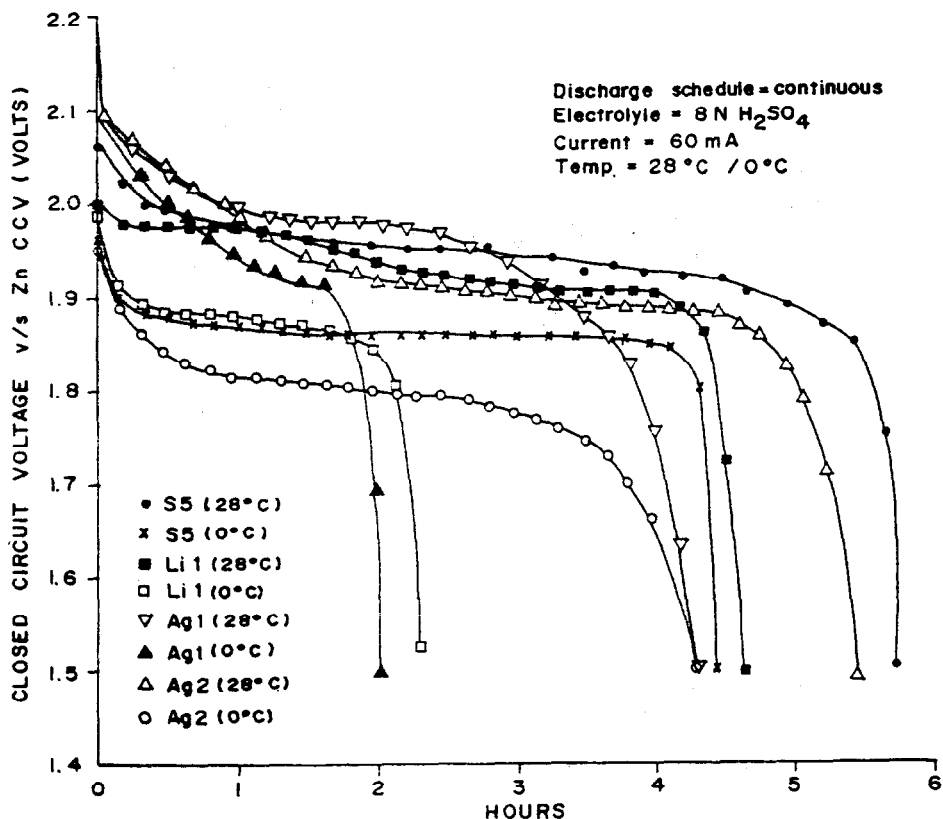


Fig. 4. Plots of closed-circuit voltage vs. time.

the opposite trend. Table 6 reveals that percentage utilization is higher in intermittent discharge at 10 Ω as compared with continuous discharge at 10 Ω . The discharge data presented in Table 6 reveal the consistency in performance of Ag-2-MnO₂, V-MnO₂, and Li-2-MnO₂. All three samples exhibit higher capacity than the molybdenum-doped sample S₅. Following Tye [14], an attempt was made to correlate the percentage theoretical capacity with the total time of discharge in the case of intermittent tests at 10 Ω . The total time is inclusive of recuperation time as well. Instead of taking the percentage theoretical capacity we took the percentage of expected Ah capacity as one of the parameters and this was plotted versus the square root of the number of days on test in the case of each sample (see Fig. 8). This figure shows that the linearity mentioned by Tye [14] is exhibited by almost all the samples except for a slight scatter in the values of V-MnO₂ and Mo-MnO₂ (S₂). The square-root-time dependence of capacity yield is indicative of a diffusion-controlled reaction. Further confirmation of this is found in the impedance spectroscopy data obtained with the doped β -MnO₂ materials, details of which are communicated separately [15].

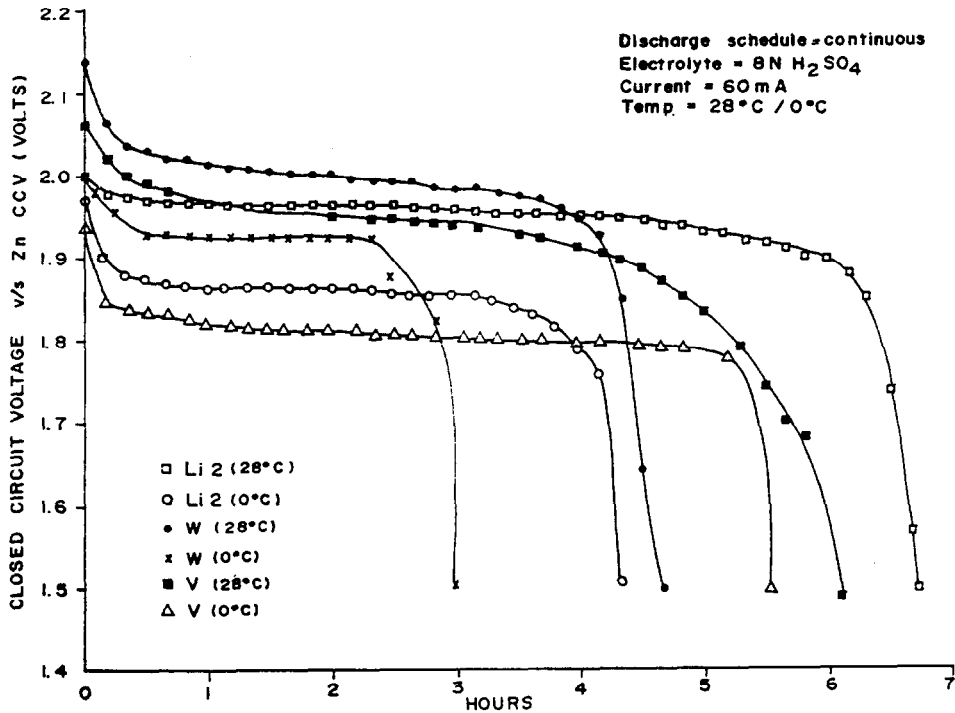
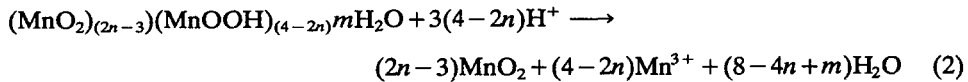
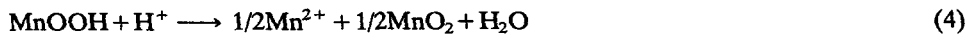


Fig. 5. Plots of closed-circuit voltage vs. time.

Further, Ruetschi *et al.* [16] are of the opinion that the Mn(III) is present in the leached liquor when strong acids are used to equilibrate with MnO₂. They suggested the following equation for the reaction:



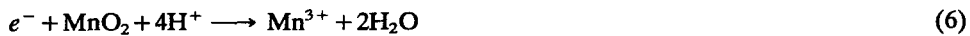
Lee *et al.* [17] have reported that the reaction proceeding on the MnO₂ surface follows the scheme:



resulting in the overall reaction:



which tallies with the equation given by Valand and Coleman [4] for a two-electron change. The equation given by them for a one-electron change:



however, is at slight variance to the one suggested by Lee *et al.* [17]. They suggest the following scheme of reactions in which the comparative instability of Mn³⁺ is emphasized:

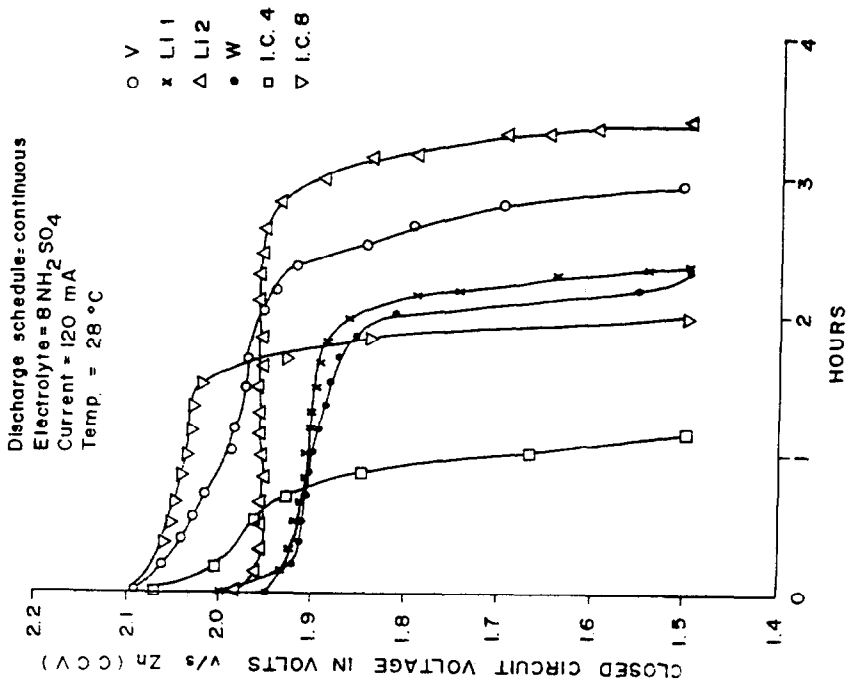


Fig. 7. Plots of closed-circuit voltage vs. time.

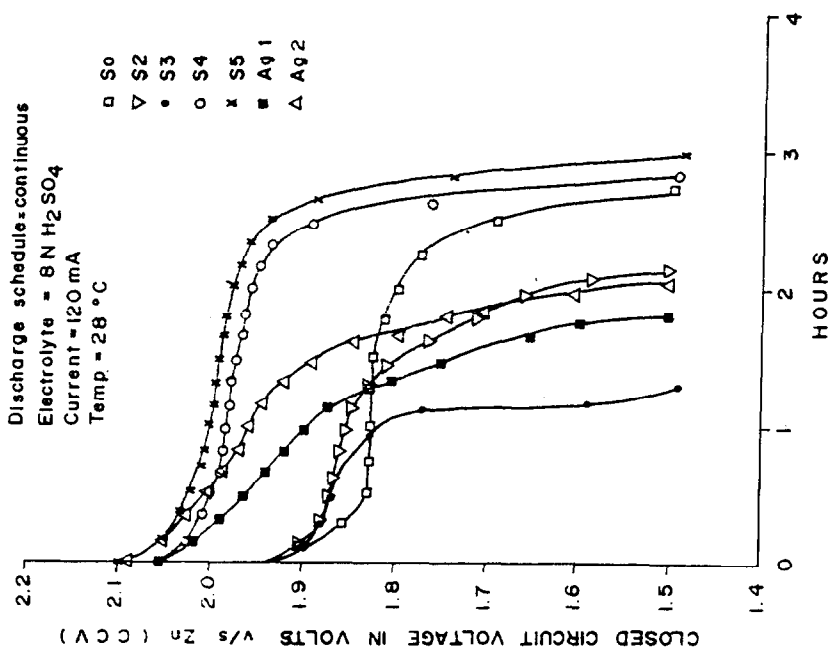


Fig. 6. Plots of closed-circuit voltage vs. time.

TABLE 6

Discharge data of continuous and intermittent tests in 8 N H₂SO₄ at 28 °C

Sample	Ah theoretical [11, 12]	Ah expected [13]	10 Ω constant resistance continuous discharge		10 Ω intermittent 0.5 h/day discharge	
			Ah observed at 1.0 V cutoff vs. Zn	Utilization (%)	Ah observed at 1.0 V cutoff vs. Zn	Utilization (%)
S ₀	0.378	0.362	0.281	78	0.339	94
S ₂	0.308	0.295	0.265	90	0.295	100
S ₃	0.377	0.361	0.313	86	0.311	86
S ₄	0.410	0.392	0.250	64	0.341	87
S ₅	0.378	0.362	0.260	72	0.325	90
Li-1	0.397	0.380	0.281	74	0.416	109
Li-2	0.383	0.367	0.344	94	0.466	127
Ag-1	0.377	0.361	0.395	109	0.283	79
Ag-2	0.356	0.341	0.320	94	0.316	93
W	0.385	0.369	0.250	68	0.241	65
V	0.343	0.329	0.375	114	0.339	103

TABLE 7

Theoretical (maximum) electrochemical capacity, C_w

Sample	Ah g ⁻¹ (Ruetschi) [11]	Ah g ⁻¹ (Atlung) [12]
S ₀	0.297	0.298
S ₂	0.242	0.187
S ₃	0.296	0.275
S ₄		0.321
S ₅	0.297	0.284
Li-1		0.311
Li-2	0.301	0.296
Ag-1	0.295	0.262
Ag-2		0.280
W	0.302	0.294
V	0.269	0.218



In the present investigation, however, Mn³⁺ was found to be present in trace quantities. However, total manganese in the electrolyte after the discharge was determined in the case of each sample and the quantities obtained are presented in

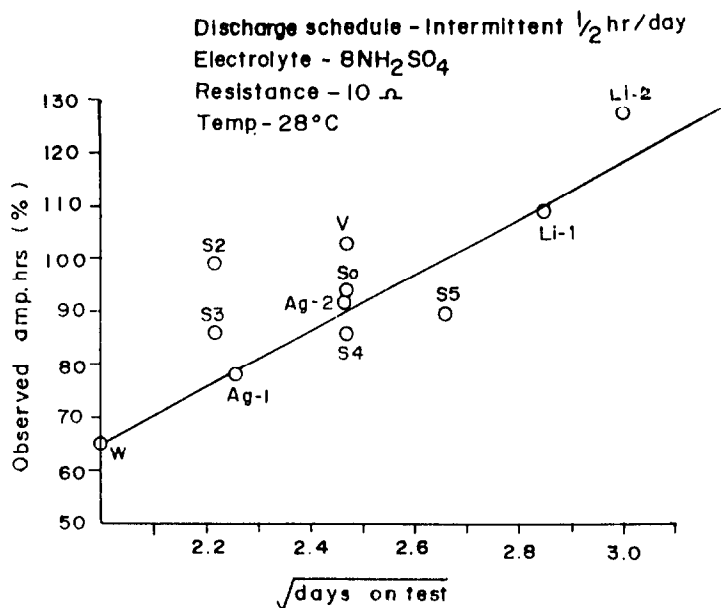


Fig. 8. Plot of observed ampere-hours vs. $\sqrt{\text{days on test}}$.

TABLE 8

Amount of manganese and moles of manganese in the electrolyte after discharge (60 mA), 8 N H_2SO_4 at room temperature (28°C)

Sample	Moles of Mn in the electrolyte after discharge	g Mn in the electrolyte after discharge
S ₀	0.012	0.68
S ₂	0.012	0.68
S ₃	0.013	0.71
S ₄	0.014	0.79
S ₅	0.014	0.75
Li-1	0.011	0.59
Li-2	0.012	0.64
Ag-1	0.014	0.76
Ag-2	0.018	1.01
W	0.006	0.36
V	0.015	0.83

Table 8. This Table reveals that 1×10^{-2} mol of manganese comes down in the electrolyte after ~ 6 h of discharge and this order of magnitude of total manganese is seen in the case of all samples belonging to molybdenum family as well as the lithium and silver families, the only exception being tungsten where the total manganese getting dissolved is of the order of 6×10^{-3} mol.

TABLE 9

X-ray crystallographic and pycnometric density data of samples

Sample	Crystal system	Lattice parameters		Cell volume [11] (V_{nm^3})	XRD density [11] ^a ($g\ cm^{-3}$)	Pycnometric density [10] ^b ($g\ cm^{-3}$)	Tap density (200 taps) [18] ($g\ cm^{-3}$)
		$a=b$ (nm)	c (nm)				
S ₀	tetragonal	0.4382	0.2864	5.50	5.23	4.31	2.64
S ₂	tetragonal	0.4372	0.2895	5.53	5.08	4.41	2.00
S ₃	tetragonal	0.4363	0.2875	5.47	5.22	4.21	2.77
S ₄	tetragonal	0.4400	0.2873	5.56	5.11	4.39	2.63
S ₅	tetragonal	0.4387	0.2862	5.52	5.19	4.17	2.77
Li-1	tetragonal	0.4094	0.2872	5.58	5.18	4.31	2.94
Li-2	tetragonal	0.4389	0.2882	5.55	5.18	4.40	2.77
Ag-1	tetragonal	0.4413	0.2863	5.57	5.15	3.96	2.38
Ag-2	tetragonal	0.4382	0.2872	5.52	5.24	4.31	1.85
W	tetragonal	0.4379	0.2859	5.48	5.25	4.16	2.38
V	tetragonal	0.4448	0.2871	5.67	4.97	4.21	2.27

^aBy using mol. wt. calculated on the basis of Ruetschi formula [11]: $Mn_{(1-x-y)}^{4+}Mn_y^{3+}O_{(2-4x-y)}^{2-}OH_{(4x+y)}^-$.

^bPycnometric density [10] in vacuum with kerosene at 40 °C.

Conclusions

The results indicate that the molybdenum-doped sample S₅ containing the least amount of molybdenum yields the best performance from amongst the molybdenum-doped family of samples when the electrochemical evaluation is carried out under constant current of 60 and 120 mA in H₂SO₄ electrolyte. The maximum discharge time is delivered by the Li-2, Ag-2 and V-MnO₂ samples. The performance of V-MnO₂ is well sustained even when the discharge is carried out at 0 °C. The Li-2 sample shows a higher efficiency in both the discharge regimes. On the other hand, the efficiency of S₅, V and Ag-2 decline perceptibly under high current drain (120 mA). The efficiencies of all the samples decrease when discharge is carried out at 60 mA at 0 °C. Samples S₅, Li-2, Ag-2, and V-MnO₂ continue to perform well when the discharge is carried out through a fixed resistance of 10 Ω. The discharge times obtained both on continuous and intermittent tests, are higher than the rest of the samples, Li-2 performing best throughout.

The observed electrochemical activity (performance) does not exhibit a direct correlation with the vacancy fraction. The percentage utilization is higher with intermittent discharge at 10 Ω as compared with continuous discharge at 10 Ω. There is a consistency in performance of Ag-2-MnO₂, V-MnO₂ and Li-2-MnO₂. All the three samples perform slightly better than molybdenum-doped sample S₅. The empirical linear relationship between percentage theoretical capacity and the square root of days on test holds good even in the case of a planar/porous electrode. The square-root-time dependence of capacity yield is indicative of a diffusion-controlled reaction.

References

- 1 G.W. Vinal, *Primary Batteries*, Wiley, New York, 1960, pp. 32–40.
- 2 W.C. Vosburg, M.J. Pribble, A. Kozawa and A. Sam, *J. Electrochem. Soc.*, *105* (1958) 1–4.
- 3 T. Valand, *J. Power Sources*, *1* (1976/77) 65–71.
- 4 T. Valand and J.R. Coleman, The Zinc–Manganese dioxide sulfuric acid battery, *DREO Technical Note No. 74-31*.
- 5 Coleman *et al.*, *US Patent No. 3 939 010* (Feb. 17, 1976).
- 6 M.W. Rophael, T.A. Bibawy, L.B. Khalil and M.A. Malati, *Chem. Ind.* (6 Jan.) (1979) 27.
- 7 J.P. Brenet, M. Cyrankowska, G. Ritzler, R. Saka and K. Traore, in A. Kozawa and R.J. Brodd (eds.), *Proc. Symp. Manganese Dioxide, Cleveland, OH, USA*, Union Carbide Corp., I.C. Sample Office, 1975, p. 274 (retyped text).
- 8 K. Takahashi, *Electrochim. Acta*, *26* (1981) 1467.
- 9 A. Kozawa, in K.V. Kordesch (ed.), *Batteries – Manganese Dioxide*, Vol. 1, Marcel Dekker, New York, 1974, p. 497.
- 10 A. Kozawa, in A. Kozawa and R.J. Brodd (eds.), *Proc. Symp. Manganese Dioxide*, Vol. 1, Union Carbide Corp., I.C. Sample Office, 1975, p. 470.
- 11 P. Ruetschi, *J. Electrochem. Soc.* *131* (1984) 2737.
- 12 S. Atlung and T. Jacobsen, *Electrochim. Acta*, *26* (1981) 1447.
- 13 R. Huber, in K.V. Kordesch (ed.), *Batteries – Manganese Dioxide*, Vol. 1, Marcel Dekker, New York, 1974, p. 137.
- 14 F.L. Tye, in M. Barak (ed.), *Primary Batteries for Civilian Use*, Electrochemical Power Sources, Peter Peregrinus, London, 1980, pp. 50–150.
- 15 B.D. Desai, F.S. Lobo and V.N. Kamat Dalal, *J. Appl. Electrochem.*, in press.
- 16 P. Ruetschi and R. Giovanoli, *J. Appl. Electrochem.*, *12* (1982) 109–114.
- 17 J.A. Lee, W.C. Maskell and F.L. Tye, *J. Electroanal. Chem.*, *110* (1980) 145–158.
- 18 T. Matsumura, in A. Kozawa and R.J. Brodd (eds.), *Proc. Symp. Manganese Dioxide*, Vol. 2, Union Carbide Corp., I.C. Sample Office, 1980, p. 596.